Neuroanatomical Circuits in the Mouse Taste System

David A. Girard, Mark C. Whitehead
UCSD SOM Department of Surgery

Purpose

The aim of the project was to map connections of the reticular formation and of the nucleus of the solitary tract (NST) that are involved in lingual and orofacial motor activity, swallowing, and salivation. These connections were established in a mouse model using injections of the neuroanatomical marker cholera toxin subunit B (CTb) placed into specific sites in the medulla.

CTb is a marker taken up by neuronal elements within the region of the brain injected with the marker. CTb has the ability to label and localize neuronal cell bodies distant from the site of brain injection whose axons terminate on the neurons within the injection site. The marker also labels the neuron's own efferent axonal endings terminating elsewhere. It accomplishes this based on its ability to be transported by a neuron's retrograde as well as anterograde transport mechanisms. Using this marker applied to specific nuclei, one can identify that brain region's afferent inputs from neurons in other brain regions (nuclei) as well as the neuron's own projections to other, e.g., "downstream", brain regions..

The pathways explored in the present limited series of experiments are those believed to interconnect the NST and nearby sites in and near the RF. The pathways involve the salivatory nucleus, and/or CN V, VII, and XII motor nuclei. These pathways have been documented for several rodential species (e.g., hamster, Beckman and Whitehead, 1991; rat, Halsell and Travers, 1996), but have not been described in the mouse with conventional neuroanatomical tracers. The mouse model, in taste research is rapidly developing insights into the molecular basis of neural coding using transgenic material (e.g., Nelson et al., 2001) that can best be interpreted with an

understanding of the types and locations of neurons comprising the taste circuits in that species. The present study is an effort toward understanding these circuits not yet fully characterized in the mouse. Localization of neuroanatomical tracer placement and of neurons labeled with tracer by retrograde transport and axonal endings labeled by anterograde transport was facilitated by reference to a cytoarchitectonic atlas of the brain stem (Paxinos et al., 2001) and of the NST (Whitehead and Finger, 2008) the mouse.

These cases were presented at the NIH Poster Presentation at UCSD School of Medicine in January 2011 (Girard and Whitehead, 2011).

Methods

4 mice were anesthetized with ketamine/xylazine. Each injection was named according to the order in which they were injected from CTb 3 to CTb 6. The occipital bone was removed with rongeurs and the midline cerebellum aspirated to expose the dorsal surface of the medulla and caudal pons. The RF and NST were approached by surgically exposing the medulla and targeting the rostral RF and the NST based on their locations ventral and ventromedial to the rostral pole of NST and relative to landmarks, e.g., blood vessels and distances from the area postrema visible on the dorsal surface of the medulla. RF localization was aided further by using coordinates in the Paxinos and Franklin (2001) mouse atlas. CTb injections were made by iontophoresis in uL quantities via micropipettes into desired regions of the medulla.

Animals survived 24-72 hours after CTb injections, the blood flushed with phosphate-buffered saline, and the animals perfused transcardially with 4% paraformaldehyde in phosphate

buffer. The brain was blocked by transverse cuts perpendicular to its long axis and to the surface on which its ventral aspect rests. The blocked tissue was stored overnight in 40% sucrose.

After paraformaldehyde perfusion, transverse sections of the medulla were immunocytochemically reacted with goat anti-CTb 1:10000 primary antibody overnight on a rotating shaker. Bound antibody was then revealed with biotinylated rabbit anti-goat IgG secondary antibody for 1 hour, followed by reaction in 0.3% hydrogen peroxide and diaminobenzidine for 4 minutes. For comparison to the atlas, sections were counterstained with Giemsa.

Observations of label in relation to brain stem nuclei were made by light microscopy and by relating the locations of label to identified nuclei evident in the counterstain and by reference to the relevant, comparable section in the atlas (Paxinos and Franklin, 2001). Photomicrographs of the injection sites and of the transported label were taken (see, e.g., Figure 2). Notes were taken of the observations of label locations. These qualitative observations are summarized below. They are intended to facilitate subsequent detailed plots of some of the data by others, an example of which is shown in Figure 1. The present observations are further intended to inform additional studies to confirm and refine the observations and to achieve a larger 'n' and statistical rigor.

Results

CTb 3 injection was large and hit the parvocellular RF and intermediate RF. There were retrogradely-labelled cell bodies and anterogradely labeled axonal endings in the ventral NST and in the RF. Plots of this labeling pattern are shown in Fig. 1. This figure is excerpted from a paper submitted for publication (Ganchrow et al., 2013). The plot shows a subset of the results I observed, specifically the reciprocal interconnection between the rostral (gustatory) NST and the subjacent RF. In addition, there was anterograde labeling in nucleus ambiguus and linear nuclei, and in motor XII, dorsolateral NST, and caudal RF (not depicted). Rostrally there was labeling in motor V, rostral RF, and motor VII. Motor X was unlabeled. This latter labeling pattern will be verified in future experiments and become part of a larger data set contributing to an expanded study and a future publication.

CTb 5, a second injection of RF was small and ventral to the rostral NST. Retrograde-labeled cells were in ventral NST and RF. There was sparse anterograde labeling of endings in nucleus ambiguus. Endings were found caudally in motor XII, ventral NST, and RF. Rostrally, endings were found in salivatory nucleus, motor V, motor VII and RF. Motor X was unlabeled.

CTb 4 injection was medium-sized in the caudal-medial NST. Retrograde-labeled cells were in the medial NST. Synaptic endings were found in the lateral NST bilaterally, motor X bilaterally, intermediate-medial NST, nucleus ambiguus and its surrounding RF, and lateral parabrachial nucleus (PBN). No endings were found in the rostral NST or in the salivatory nucleus.

CTb 6 was a small injection in the intermediate-medial NST, i.e., rostral to that in CTb4. Labeled cells were in the medial NST rostrally. Endings were found caudally and rostrally within the NST as well as rostrally in the inferior salivatory nucleus. No labeling was found in motor X, in the extreme rostral NST, nucleus ambiguus, or parabrachial nucleus (PBN).

The following figures are examples of the data collected and represent part of my contribution to the manuscript submitted. The plot itself was generated by another author, but the case itself was produced by myself and Dr. Whitehead. In addition, qualitative descriptions of transported label from all 4 cases were added to the results in the relevant sections of the text of the submitted manuscript (Ganchrow et al., 2013).

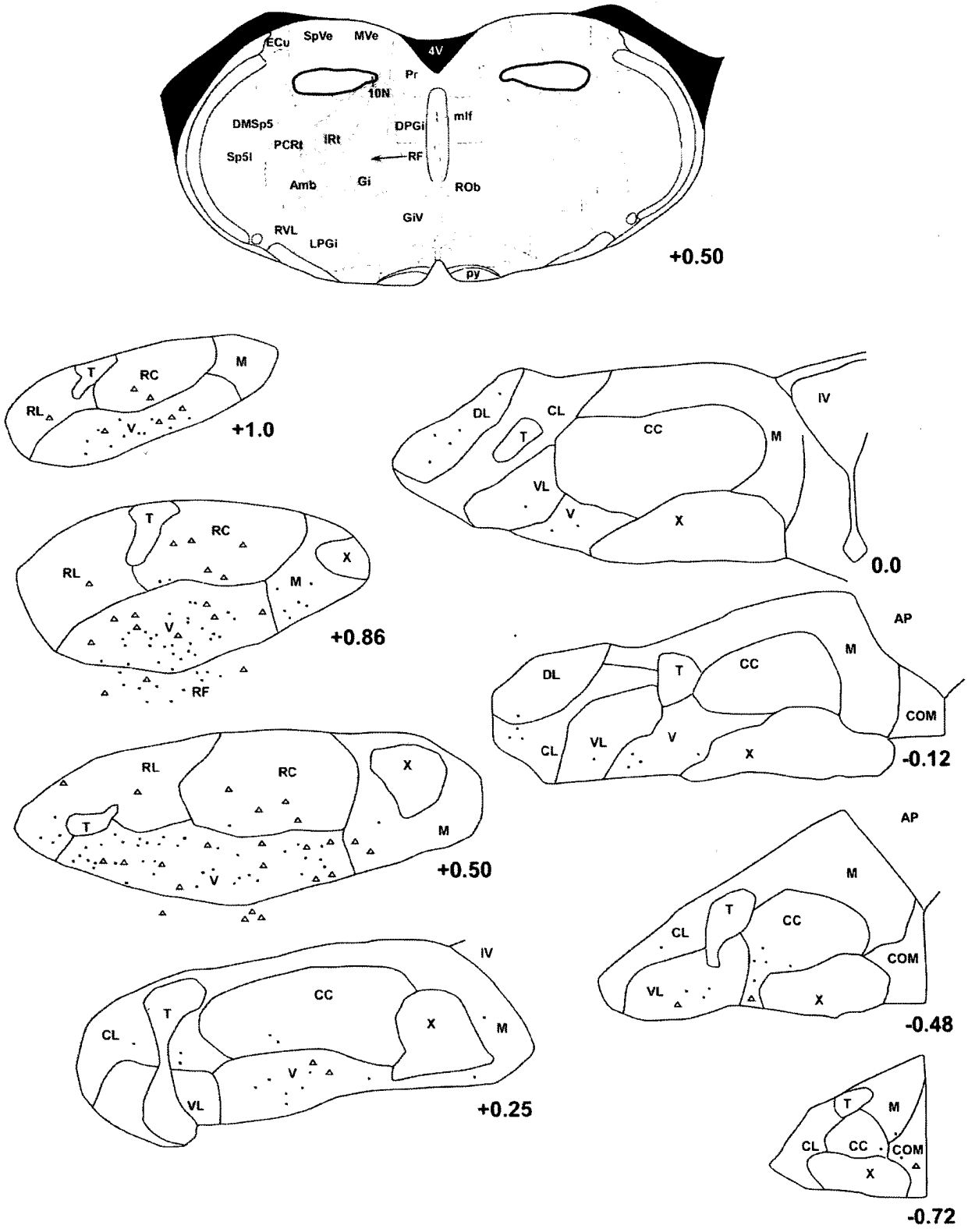
ECu
SpVe
MVe
4V
Pr
10N
DMSp5
DPGi
mlf
PCRt
IRt
Sp5I
RF
Amb
Gi
ROb
GiV
RVL
LPGi
py
+0.50
RL
T
RC
M
V
+1.0
DL
CL
T
CC
M
IV
VL
V
X
0.0
RL
T
RC
X
M
V
RF
+0.86
AP
DL
T
CC
M
COM
CL
VL
V
X
-0.12
RL
RC
X
T
M
V
+0.50
AP
M
T
CL
CC
COM
VL
X
-0.48
IV
CC
CL
T
X
M
V
VL
+0.25
T
M
CL
CC
COM
X
-0.72

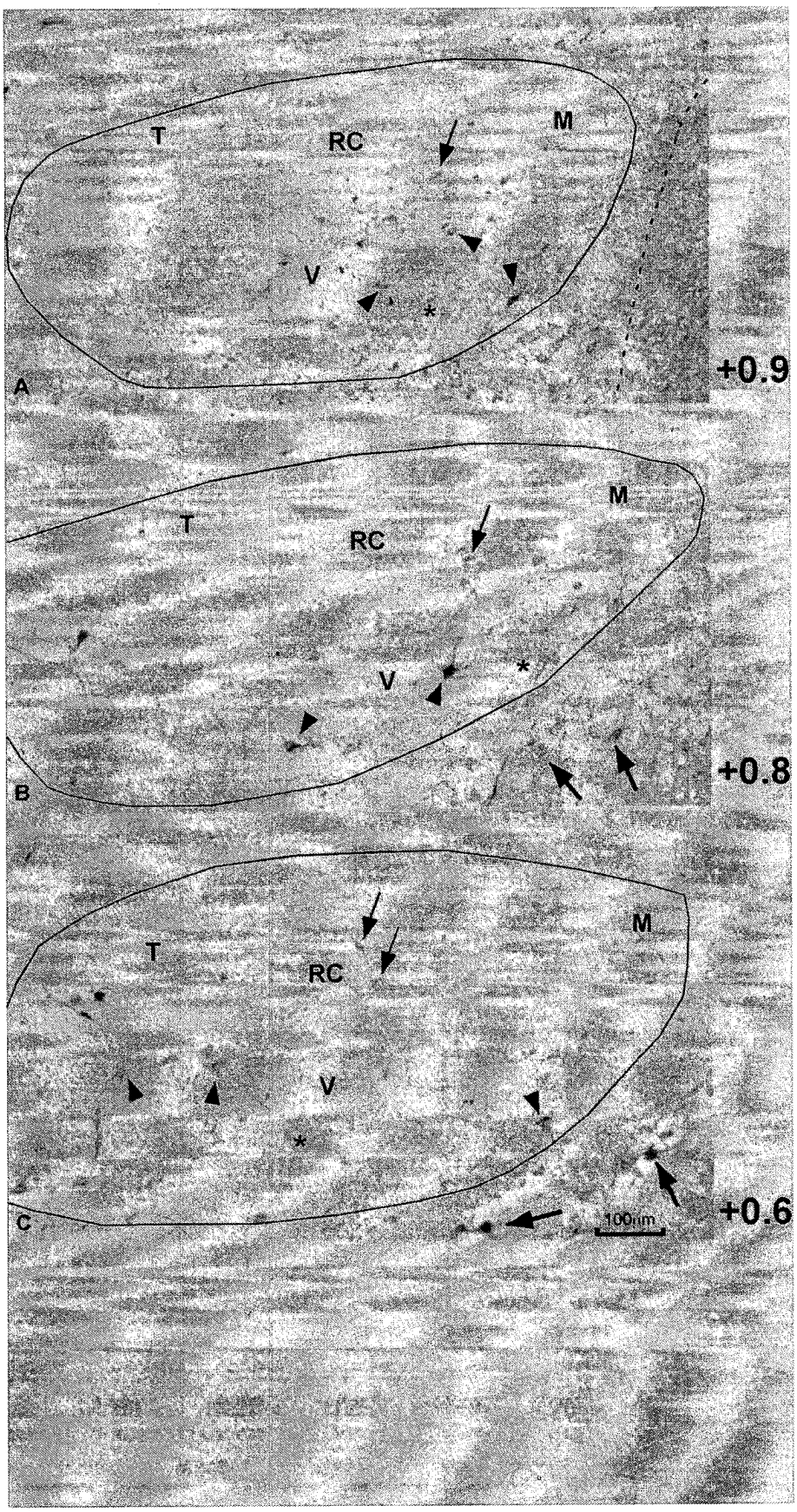
T
RC
M
V
*
A
+0.9
T
RC
M
V
*
B
+0.8
T
RC
M
V
*
C
100µm
+0.6

List of Abbreviations

Amb	ambiguus nucleus
AP	area postrema
C	central canal
Ce	central subnucleus (of NST)
CC	caudal central subdivision (of NST)
CI	caudal interstitial nucleus of the medial longitudinal fasciculus
CL	caudal lateral subnucleus (of NST)
COM	commissural subnucleus (of NST)
CT	chorda tympani nerve
Cu	cuneate nucleus
DC	dorsal cochlear nucleus
DL	dorsal lateral subnucleus (of NST)
DMSp5	dorsomedial spinal trigeminal nucleus
DPGi	dorsal paragigantocellular nucleus
DT	dorsal tegmental nucleus
ECu	external cuneate nucleus
Gi	gigantocellular reticular nucleus
GiA	gigantocellular reticular nucleus, alpha
GiV	gigantocellular reticular nucleus, ventral part
Gr	gracile nucleus
GrC	granular layer of cochlear nuclei
In	intercalated nucleus of medulla
IRt	intermediate reticular nucleus
K	Kölliker-Fuse nucleus (of pons)
LC	locus coeruleus
Li	linear nucleus

LPGi	lateral paragigantocellular nucleus
LRt	lateral reticular nucleus
LRtPC	lateral reticular nucleus, parvicellular part
LVe	lateral vestibular nucleus
M	medial subnucleus (of NST)
m5	motor root of the trigeminal nerve
mlf	medial longitudinal fasciculus
MdD	medullary reticular nucleus, dorsal part
MdV	medullary reticular nucleus, ventral part
MVe	medial vestibular nucleus
MVeMC	medial vestibular nucleus, magnocellular part
MVePC	medial vestibular nucleus, parvocellular part
NST	nucleus of the solitary tract
P7	perifacial zone
Pa5	paratrigeminal nucleus
PBN	parabrachial nucleus (of pons)
PBN-L	parabrachial nucleus, lateral division
PBN-M	parabrachial nucleus, medial division
PCRt	parvocellular reticular nucleus
PCRtA	parvocellular reticular nucleus, alpha
PMn	paramedian reticular nucleus
PnC	pontine reticular nucleus, caudal part
PPy	parapyramidal nucleus
Pr	prepositus nucleus
Pr5DM	principal sensory trigeminal nucleus, dorsomedial part
Pr5VL	principal sensory trigeminal nucleus, ventrolateral part
py	pyramidal tract
RAmb	retroambiguus nucleus
RC	rostral central subnucleus (of NST)

RF	reticular formation (of medulla)
RL	rostral lateral subnucleus (of NST)
RMg	raphe magnus nucleus
Ro	nucleus of Roller
ROb	raphe obscurus nucleus
RPa	raphe pallidus nucleus
RVL	rostroventrolateral reticular nucleus
SO	superior olive
Sp5C	spinal trigeminal nucleus, caudal part
Sp5I	spinal trigeminal nucleus, interpolar part
Sp5OVL	spinal trigeminal nucleus, oral part
SpVe	spinal vestibular nucleus
Su5	supratrigeminal nucleus
T	solitary tract
T5	spinal trigeminal tract
V	ventral subnucleus (of NST)
VCP	ventral cochlear nucleus, posterior part
VL	ventral lateral subnucleus (of NST)
4V, or, IV	4^{th} ventricle
5N	motor trigeminal nucleus
7N	facial nucleus
10N, or, X	vagal motor nucleus
12N, or, XII	hypoglossal nucleus

Figure Legends

Fig. 1. Qualitative plots of retrogradely labeled NST, and, medullary reticular formation (RF) projection cells immediately subjacent to the NST (open triangles), and, the RF projection field in the NST (dots), after CTb injection into the medullary RF [uppermost schematic, shaded diagonal lines; schematic adapted from Paxinos and Franklin (2001)]. The injection site extends from a medial sector of medial vestibular nucleus (Mve) ventrally to above ambiguus nucleus (Amb), and does not invade NST. Rostral to the obex, retrogradely labeled somata in the NST subnuclei predominate in V, and to a lesser degree in RC. Along the entire rostrocaudal extent of the NST, fewer labeled somata are evident in RL, M and VL. RF terminal projection field endings in the NST predominate in V, and to a lesser degree in RC, CC, RL, CL, DL and M. Retrogradely labeled cells and terminal endings also are evident in the RF subjacent to the V subnucleus of NST. See List of Abbreviations.

Fig. 2. Photomicrographs of retrogradely labeled NST somata, and projection field terminations in the NST (outlined) after CTb injection into the medullary reticular formation (rf. same case, Fig. 1).The dorsal portion of the injection site (dashed line in A) medially borders the medial subnucleus (M) of NST. In A-C, retrogradely labeled NST somata predominate in V (arrowheads) and are larger than the more sparsely labeled cells in RC (thin arrows). Labeled reticular formation projection field endings (asterisks in A-C) are scattered in subnucleus V of the NST. Retrogradely labeled cells also are present in the reticular formation (thick arrows in B and C) immediately subjacent to the V subnucleus of the NST. Sections B and C are lightly Nissl-counterstained. See List of Abbreviations.

Discussion

The murine model has been important in understanding neurobiology on the molecular as well as tissue level (e.g., Nelson et al, 2001). An important reason for this is the similarity in

brainstem function and architecture between the mouse and human, another is the advent of transgenics and widespread use of the murine model in that scientific discipline. There has been recent growth of information regarding the neuronal organization of the taste pathway, such as different tastes localizing to different specific cell types within the taste bud (Nelson et al. 2001). And with the recent growth in knowledge of how gustatory information is differentially encoded in the brain, there has been recent demand for elucidation of the exact pathways in the brainstem. As all afferent taste information projects to the NST, to understand these multiple taste circuits, a map of NST connections must be established. This map may be used for interpretation of neuroanatomic and genetic marker data from transgenic mice. The data generated from these CTb injections contributes to the data set for mapping the taste circuits in the mouse.

The RF injections, CTb 3 and 5, both had significant synaptic endings in motor V, VII, and XII, which are the general somatic efferent (GSE) cranial nerves. CTb5 also labeled endings in the inferior salivatory nucleus, which has general visceral efferent (GVE) function. Since our RF injection sites label axonal endings in these motor nuclei, and cell bodies the NST, these RF sites likely are an important "pre-motor" connection in orchestrating feeding behavior. The RF sites are intermediate in a pathway leading from the sensory NST to the oromotor outflow (Beckman and Whitehead, 1991; Halsell et al., 1996). Some of the connections observed in these cases are the first evidence observed in the mouse brainstem with the marker CTb. They validate circuits gleaned from a recent study of the mouse gustatory pathways using transynaptic transport of a novel fluorescently tagged virus strain (Zaidi et al., 2008).

The NST injections, CTb 4 and 6, differ in size and rostrocaudal location. CTb4, the larger one, at a caudal general viscerosensory (non-gustatory) level, verifies a projection from the NST to the RF, and, uniquely, connections to motor X (GVE). Its lateral PBN connection is consistent

with its general viscerosensory nature and caudal NST location. CTb6, by contrast, is more rostral than CTb4, and is reciprocally connected to the rostral pole of the NST (gustatory); it connects directly with the salivatory nucleus.

References

1. Beckman ME, Whitehead MC (1991) Intramedullary connections of the rostral nucleus of the solitary tract in the hamster. Brain Res 557:265-279.

2. Ganchrow D, Ganchrow JR, Cicchin V, Bartel DL, Kaufman D, Girard D and Whitehead MC (2013) The nucleus of the solitary tract in the C57BL/6J Mouse: Subdivisions, Chorda Tympani Nerve projections and Brain Stem Connections. Submtted, Journal of Comparative Neurology.

3. Girard, D., Whitehead MC. NIH Poster Presentation 1/2011, Neuroanatomical Circuits in the Mouse Taste System

4. Halsell CB, Travers SP, Travers JB (1996) Ascending and descending projections from the rostral nucleus of the solitary tract originate from separate neuronal populations. Neuroscience 72:185-197.

5. Nelson G., Hoon MA, Chandrashekar J, Zhanf Y, Ryba NJP, Zuker CS (2001) Mammalian sweet taste receptors. Cell 106: 381-390

6. Paxinos G, Franklin KBJ (2001) The mouse brain in stereotaxic coordinates. 2nd edition. New York: Academic Press

7. Zaidi FN, Todd K, Enquist L, Whitehead MC (2008) Types of taste circuits synaptically linked to a few geniculate ganglion neurons. J Comp Neurol 511:753-772.